Final report

1. Project details

Project title	Boosting Economic Electrolyzer Stack Technology 2 (BEEST2)
File no.	64021-2074
Name of the funding scheme	EUDP
Project managing company / institution	Technical University of Denmark, Department of Energy Conversion and Storage (DTU)
CVR number (central business register)	30060946
Project partners	Green Hydrogen Systems (GHS), Aalborg University (AAU)
Submission date	30/09/2025

2. Summary

Project summary:

BEEST2 aimed at developing a more efficient and durable alkaline water electrolysis (AWE) stack to lower green hydrogen cost and enable PtX technologies and fossil fuel phase out. Combining new materials, advanced electrochemical testing, and multi-physics simulations accelerated innovations in electrode and stack design.

BEEST2 accelerated electrode optimization and degradation analysis by employing a novel methodology to separate electrode contributions in AWE cell testing at DTU. Hydrogen and oxygen evolution catalysts and effective electrode architectures were identified, achieving 1 A/cm² with only 1.75 V full cell voltage at 80 °C, 30 wt% KOH, surpassing EU performance targets for 2030. The employed anodes showed negligible degradation over 1000 h of continuous operation, but revealed structural and compositional changes upon post-test evaluation, requiring longer-term degradation studies to assess their industrial potential. Intermittent operation proved detrimental to the anodes due to interface instability between the catalyst coating and Ni support, highlighting the need for further interface tuning.

A world-leading computational fluid dynamics model of an AWE was developed at AAU, capable of capturing performance and bubble dynamics. The simulations inspired the inclusion of micro-cracks on the surface of the diaphragm to induce the formation of hydrogen bubbles on one side and oxygen bubbles on the other, thus reducing product gas cross-over. While GHS first expressed commercial interest in this invention, the idea of patenting was finally dropped.

Overall, BEEST2 supported the training of 1 PhD and yielded 8 peer reviewed publications and 1 invention disclosure.

Projektresumé:

BEEST2 havde til formål at udvikle en mere effektiv og holdbar alkalisk vand elektrolyse (AWE) for at sænke omkostningerne ved grøn brint og muliggøre PtX teknologier og udfasning af fossile brændstoffer. Kombinationen af nye materialer, avanceret elektrokemisk testning og multiphysik simuleringer accelererede innovationer i elektroder og stack design.

BEEST2 accelererede elektrodeoptimering og nedbrydningsanalyse ved at anvende en ny metode til at adskille elektrodebidrag i AWE-celletestning i DTU. Hydrogen- og iltudviklingskatalysatorer og effektive elektrodearkitekturer blev identificeret, der opnåede 1 A/cm² med kun 1,75 V fuld cellespænding ved 80 °C, 30 vægt% KOH, hvilket overgik EU's præstationsmål for 2030. De anvendte anoder viste ubetydelig nedbrydning over 1000 timers kontinuerlig drift, men afslørede strukturelle og sammensætningsmæssige ændringer ved evaluering efter testen, hvilket kræver længerevarende nedbrydningsstudier for at vurdere deres industrielle potentiale. Intermitterende drift viste sig at være skadelig for anoderne på grund af grænsefladeustabilitet mellem katalysatorbelægningen og Ni-understøtningen, hvilket understregede behovet for yderligere grænsefladejustering.

En verdensførende beregningsmodel for fluiddynamik af en AWE blev udviklet i AAU, som er i stand til at registrere ydeevne og bobledynamik. Simuleringerne inspirerede til inkludering af mikrorevner på membranens overflade for at inducere dannelsen af hydrogenbobler på den ene side og iltbobler på den anden, hvilket reducerer produktgasovergang. Selvom GHS først udtrykte kommerciel interesse i denne opfindelse, blev ideen om patentering endelig droppet.

Samlet set støttede BEEST2 uddannelsen af 1 ph.d. og resulterede i 8 fagfællebedømte publikationer og 1 opfindelsesoffentliggørelse.

3. Project objectives

BEEST2 targeted the development of a next generation alkaline water electrolysis (AWE) stack by improving the efficiency, price and durability of the electrodes, using new combinations of materials and electrode architectures, along with the implementation of state-of-the-art 3D multi-physics simulations to improve the design of internal cell and stack components.

The cross-disciplinary partners in BEEST2 joined forces to (a) investigate the factors and mechanisms that limit the lifetime and efficiency of the current generation of electrolyzers, such as electrode degradation, and the flow and heat distribution within the cells and stack, (b) evaluate new materials and designs to overcome these limitations and, based on the gained insights, (c) develop technologically relevant solutions for implementation within next-generation AWE.

The specific objectives of BEEST2 were:

- To develop porous electrodes based on optimized 3D structures and applied catalytic layers that result in a cell voltage below 1.75 V at a current density of 1 A/cm2 at the laboratory scale (25 cm2).
- To develop, test and validate electrodes that show a degradation rate of less than 0.12% per 1000 h of operation at 1 A/cm2 and a temperature of (at least) 100°C at the laboratory scale (25 cm2).

- To develop 3D multi-physics simulation models at different length scales that can be leveraged to improve the design and configuration of internal cell and stack components.
- By means of 3D multi-physics simulations, optimize the distribution of the two-phase fluid flow, reactants, heat and current density within the cell active area and the stack, resulting in an improved conversion efficiency from electric power to hydrogen.

4. Project implementation

The project evolved smoothly during the first 2-2½ years with good progress on all parallel tracks and excellent collaboration amongst project partners. The development of catalysts and the targeted electrode and cell performance was very ambitious but achieved thanks to the intensive efforts and good collaboration between DTU and GHS. The development of a novel computational model was also very ambitious, but all milestones were met. The PhD student worked for the first 18 months at AAU and then transitioned to GHS in Kolding, thereby helping with knowledge transfer.

The final part and conclusion of the project was nevertheless rammed by the unfortunate bankruptcy of GHS, linked to the overall downturn experienced in the field with much slower adoption of green hydrogen in commercial applications than expected upon project start. This resulted in the need to revise the final goals of the project, abandoning the planned demonstration of the improved stack produced in the project, shifting instead resources towards a more refined assessment of electrode degradation mechanisms. The uncertainty associated with GHS' entering in-court reconstruction, necessitating project revision and transition of project management from GHS to another partner in the consortium was also the reason for the extension of the project duration and transition of the project management to DTU.

5. Project results

All of the project objectives were met, apart from the originally planned demonstration of the developed innovations within a full-scale stack and system operating under realistic conditions. A full-scale stack incorporating the most mature innovations was produced but not tested due to a necessary interruption of operations at GHS following their entering a phase of in-court reconstruction and withdrawal from the project. The project was revised at that point, shifting focus to more extensive investigations of the long-term performance evolution and degradation of the developed anodes under different operational scenarios to help further mature this critical stack component.

The technological results obtained within BEEST2 fall within three categories, i) electrocatalysts and electrodes, ii) Multiphysics simulations, and iii) stack design, as described below.

Electrocatalysts and electrodes:

Electrocatalyst development

HER catalysts were developed using several approaches, one of the most promising being machine-learning (ML) driven optimization of Ni, Ni–W, and Ni–Mo electrodeposition. Deposition parameters such as bath pH, current density, deposition time, and temperature were optimized. Initially, 13 Ni-W coatings were prepared and tested, revealing that improved catalyst coating performance was primarily due to increased surface area rather than a boost in intrinsic activity due to the presence of tungsten. Therefore, we focused on optimizing

Ni electrodeposition alone. At first, 15 samples were prepared by Ni electrodeposition on fine Ni foam support by varying deposition parameters such as pH, current density, and deposition time over a broad range as shown in Figure 1(a–c). The electrochemical performance results of these samples were used in ML algorithms, which suggested new deposition conditions. Following this iterative process, a total of 51 Ni electrodeposited samples were synthesized and tested; their overpotentials at 100 mA.cm^{-2} shown in Figure 1(d). Using this approach, a minimum overpotential of 195 mV at 100 mA.cm^{-2} and 25 °C was achieved with just bare Ni electrodeposition as shown in Figure 1(e). Despite these promising room-temperature results, the catalysts exhibited minimal thermal activation when tested in a flow cell, Figure 1(f).

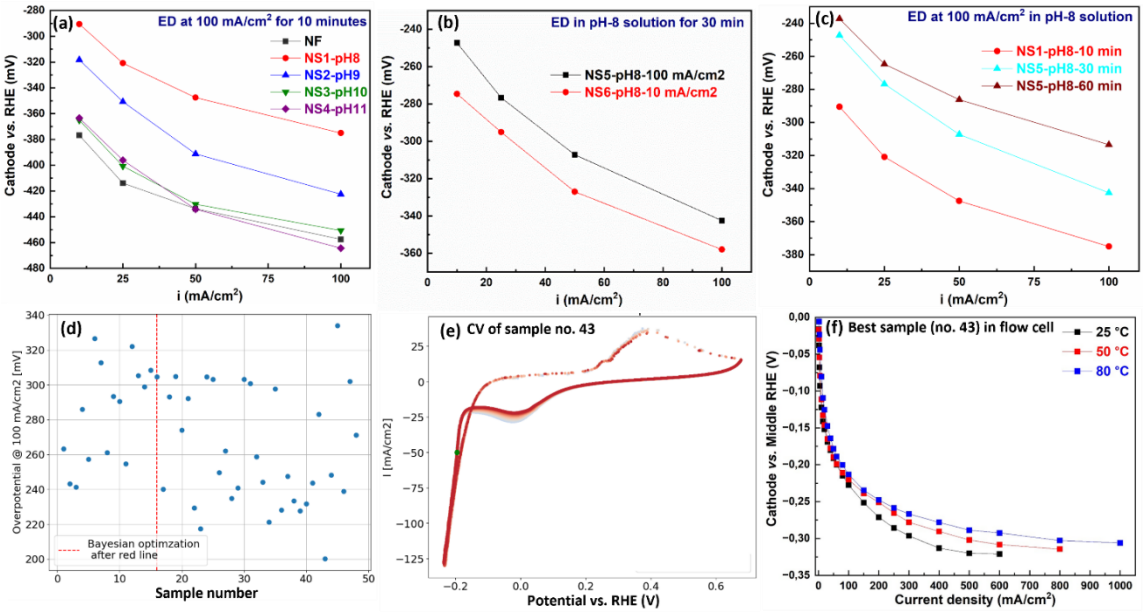

Figure 1. Electrochemical performance of Ni electrodes prepared by electrodeposition on Ni foam: (a) effect of deposition bath pH, (b) effect of deposition current, (c) effect of deposition time, (d) overpotential of all 51 samples at 100 mA.cm^{-2}, (e) cyclic voltammogram of the best-performing sample at a scan rate of 50 mV/s, and (f) performance of the best electrode at different temperatures.

A similar effort was undertaken in optimizing electrodeposition of Ni–Mo coatings using ML. The deposition current density and temperature were the most impactful parameters. The best coating achieved required only 103 mV to deliver 100 mA/cm^2 with a Tafel slope of 43 mV/dec, linked to its exceptionally high surface area of approx. 10^5 cm^2/cm^2.

In parallel, GHS was developing their own electrocatalyst coating for HER, which was evaluated under high temperature and pressure (HTP) conditions at DTU. The catalyst coating demonstrated outstanding performance, requiring only 47 mV overpotential at 100 mA/cm² (geometric) at 100 °C and 50 bar. It should be pointed out though that this value reflects the overpotential at the back side of the electrode, due to the placement of the reference electrode, which is expected to be somewhat lower than the overpotential at the front side of the electrode. When normalized to the active surface area, the catalyst exhibited an intrinsic activity corresponding to less than 80 mV at 10 mA/cm² at 100 °C which was well below milestone M2.2 “Identification of cathode catalysts with an intrinsic activity corresponding to < 0.2 V overpotential at 10 mA/cm^2 (active surface area normalized) at 100 ºC”. Since the milestone target was achieved further work was focused on anode catalyst development.

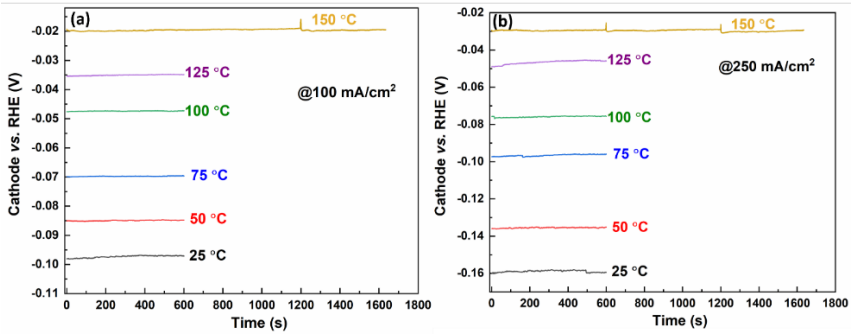

Figure 2. Electrochemical performance of HER electrocatalyst developed by GHS at 50 bar and 30wt% KOH: (a) CP at 100 mA/cm^2 and (b) CP at 250 mA/cm^2.

CoOx was initially explored as an OER catalyst due to existing knowledge of its favorable reaction kinetics from other projects.

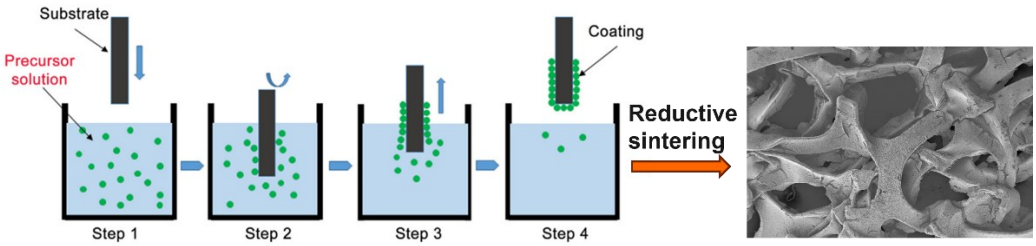

Figure 3. Schematic diagram of CoO_x/NF electrode preparation.

The catalyst was prepared by dip-coating Ni foam (NF) in a cobalt oxide slurry, followed by sintering under oxidizing–reducing conditions as shown in Figure 3. Electrochemical performance was evaluated under HTP conditions and compared against pristine NF and commercial Inconel coated NF (Inconel/NF, Alantum Corp.) as shown in Figure 4. Steady-state polarization showed strong thermal activation of CoO_x/NF, with the overpotential at 500 mA cm^{-2} decreasing from 0.394 V (25 °C) to 0.186 V (150 °C), i.e., 1.66 mV K^{-1}. Pristine NF displayed the highest thermal activation (3.39 mV K^{-1}), whereas Inconel/NF showed the lowest (0.94 mV K^{-1}). At 150 °C, CoO_x/NF and Inconel/NF show similar performance. Electrode stability was assessed at 150 °C and 45 bar by stepwise chronopotentiometry (CP) measurement cycling (10 → 100 → 250 → 500 mA cm^{-2}). NF maintained stable performance for >72 h. CoO_x/NF also showed excellent stability over 108 h (Fig. 4(e)). On the other hand, Inconel/NF showed stable performance for ~24 h, followed by progressive degradation, with a 26 mV rise in overpotential after 84 h at 500 mA cm^{-2} (Fig. 4(f)). Post-mortem SEM analysis revealed significant microstructural modifications in all electrodes (Fig. 5). Pristine NF showed formation of a porous surface layer after testing (Fig. 5(a′)). CoO_x/NF formed nanoflake-like features uniformly distributed within macropores (Fig. 5(b′)). Inconel/NF initially comprised dense spherical particles (5–50 μm) with smooth surfaces (Fig. 5(c)). After extended testing, Inconel particles developed porous corrosion shells (Fig. 5(c′)). EDS mapping confirmed leaching of Mo, Si, Nb, and Cr from the corroded Inconel surface likely causing the degradation in electrochemical performance. The key outcome of this study was the identification of CoO_x as a highly active and stable electrocatalyst for the OER, demonstrating robustness under harsher conditions (150 ºC and 45 wt.% KOH) than those targeted (100 ºC and 30 wt.% KOH).

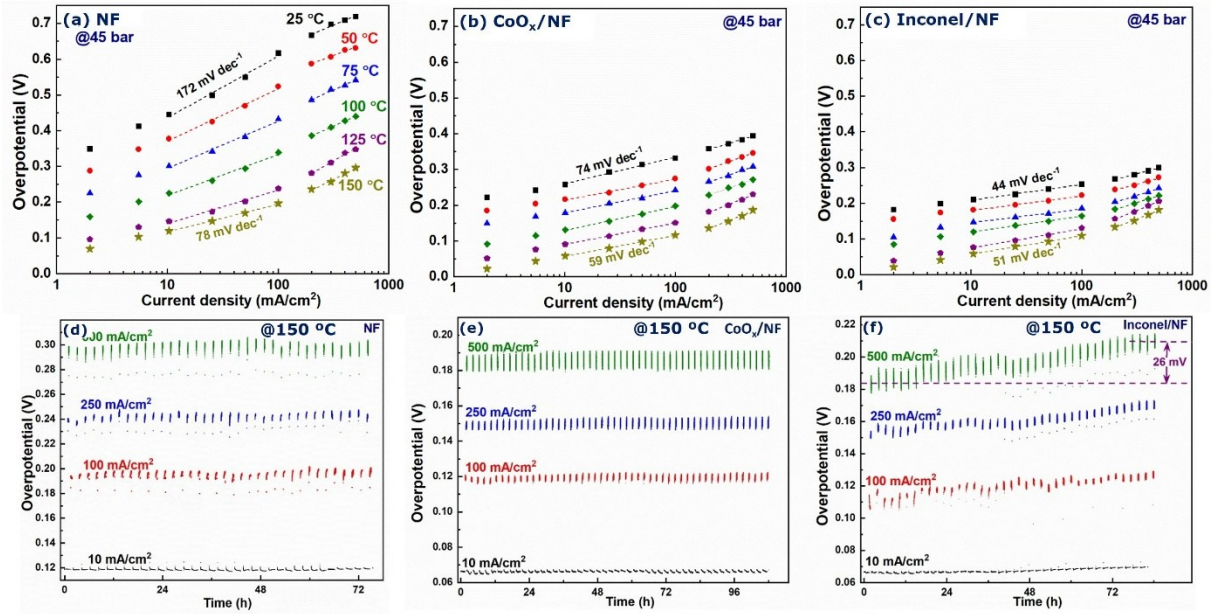

Figure 4. Tafel plots of (a) pristine NF (b) CoOx/NF and (c) Inconel/NF electrodes from 25 ºC to 150 ºC, and CP measurements of (d) pristine NF (e) CoO_x/NF and (f) Inconel/NF electrodes upon cycling current density between 10, 100, 250, and 500 mA.cm^{-2} at 150 ºC and 45 bar in 45 wt.% KOH.

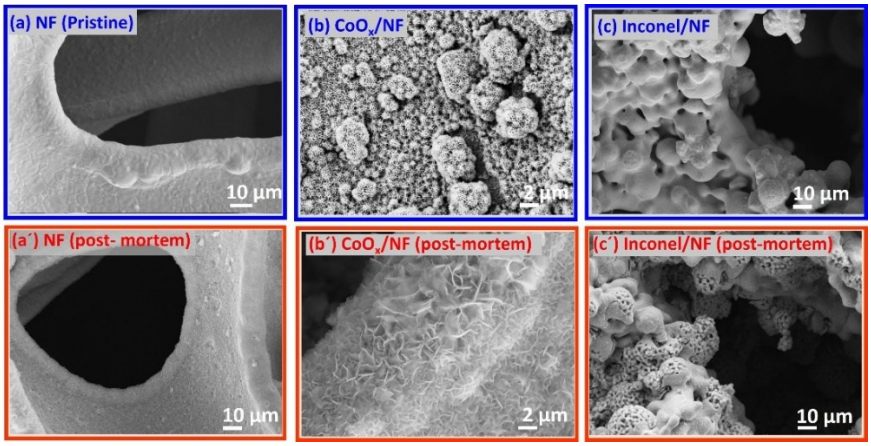

Figure 5. Electron microscopy images of (a) pristine NF, (b) CoOx/NF, and (c) Inconel/NF electrodes prior to electrochemical testing and their corresponding images after electrochemical testing are shown in (a'), (b'), and (c'), respectively.

Additional OER catalysts were explored, taking advantage of ongoing activities within the DFF project FREESLI and the DTU funded project ENERGHy, exploring oxyhydroxides and perovskites, respectively. Nickel–iron oxyhydroxide ($Ni_{1-x}Fe_xOOH$) is among the most active OER catalysts reported but typically evaluated under mild conditions (10–100 mA cm^{-2}, 10–100 h, 1 M KOH, room temperature). At DTU, we synthesized $Ni_{1-x}Fe_xOOH$ (x = 0–0.33) via a hydrothermal route and assessed its activity and stability under industrially relevant conditions (70–80 °C, 6–10 M KOH). Systematic studies were conducted in 1, 6, and 10 M KOH at 75 °C for ~30 days under stepwise increase in current (10 → 400 mA cm^{-2}, ~6 days/step) using a custom-made cell in a rig accommodating up to 12 such cells in parallel. Linear sweep voltammetry (LSV) curves showed that Fe incorporation enhanced activity, with 25 at.% Fe giving the best performance across most conditions, followed by 20 and 33 at.% Fe as shown in Figure 6 (a-c). Long-term testing revealed good activity retention in 1 M KOH at 75 °C. In contrast, higher concentrations (6–10 M KOH) led to pronounced potential

rise and rapid activity loss for Fe-containing samples. Post-mortem SEM (Figure 7) confirmed stable morphology for Fe-free electrodes, while Fe-containing samples exhibited coarsening and restructuring of the nanoflakes even in 1 M KOH. Severe coating loss and peeling were observed at 6 and 10 M KOH, indicating poor durability of the catalyst/support interface under harsher alkaline conditions. During this long-term test, measurements were intermittently interrupted to record EIS. In addition, the electrolyte volume decreased in-between manual water refilling taking place every two days, effectively increasing the KOH concentration. These factors have likely contributed to the observed degradation.

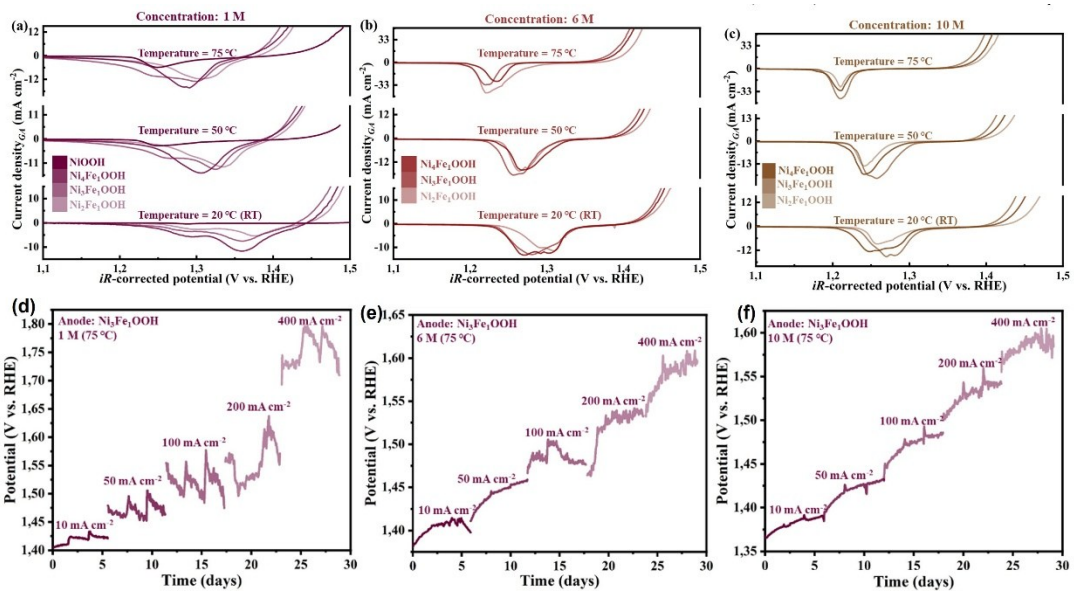

Figure 6. LSV curves of $Ni_{1-x}Fe_x$-LDH (x = 0-0.33) samples in (a) 1 M (b) 6 M and (c) 10 M KOH at 20, 50, and 75 ℃ and, long-term electrochemical stability test of Ni_3Fe_1OOH in (d) 1 M, (e) 6 M, and (f) 10 M KOH (75 ℃) at step-wise increasing current density.

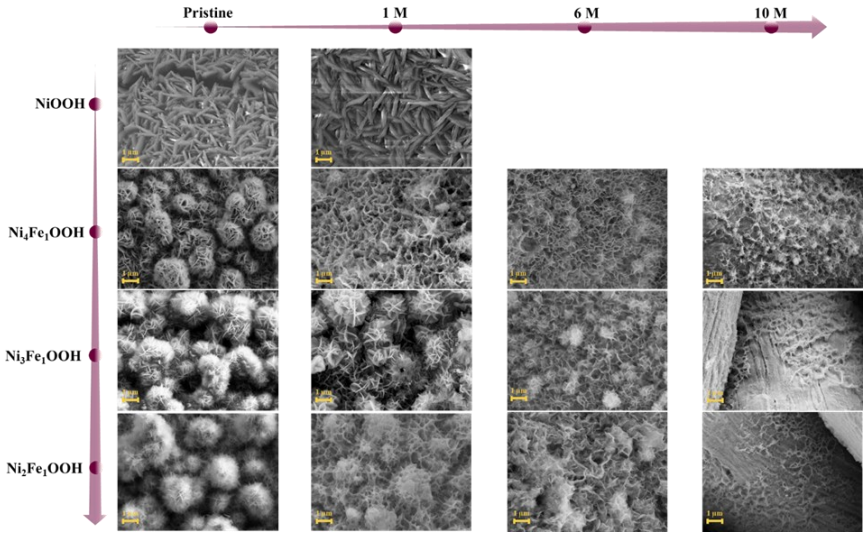

Figure 7. SEM images of the as-synthesized and ~30days tested $Ni_{1-x}Fe_x$-LDH (x = 0-0.33) samples in 1, 6, and 10 M KOH (75 ℃).

Screening a series of perovskites (chemical formula ABO_3) with A = La and/or Sr and B = Mn or Fe and/or Co, it was concluded that $LaFeO_3$ and $La_{0.6}Sr_{0.4}Fe_{0.8}Co_{0.2}O_3$ were the most active for the OER, but none of them was stable during a 200h long OER test at 75 °C, 50 bar, 10 M KOH. On the other hand, $Sr_{0.98}Ti_{0.7}Fe_{0.25}Ni_{0.05}O_3$ was found to be both very active for the OER and stable over 200h at 100 °C, 50 bar, 10 M KOH. $Ni_{1-x}Fe_xOOH$

was nevertheless selected for anode development due to the relatively facile growth of this catalyst on a Ni support.

Electrode development

An advanced experimental setup was designed with a zero-gap flow-cell holder accommodating multiple reference electrodes (REs) to separate the overpotential contributions from Anode and Cathode and to quantify the Galvani potential loss within each electrode. Since the Galvani loss reflects ionic transport resistance within the electrode, the use of multiple REs enables the evaluation of porous electrode architectures in terms of mass transport for both the Anode and Cathode. Two different RE placement configurations were implemented, as illustrated in Figure 8(a) and 8(b). In both configurations, a reversible hydrogen electrode (RHE) was positioned behind the cathode at the electrolyte inlet (denoted as R_C), while a Hg/HgO electrode was placed behind the anode at the electrolyte inlet (denoted as R_A). In Configuration 1 (Figure 8(a)), two additional RHEs were introduced, each placed in an external reservoir containing 30 wt.% aqueous KOH and connected ionically to the cathode/separator interface (denoted as R_{MC}) and the anode/separator interface (denoted as R_{MA}). Ionic contact was achieved using a microporous PES membrane strip, which was inserted between the electrode and the separator. In Configuration 2 (Figure 8(b)), a single RHE (R_M) was connected to the separator by extending a strip of the separator into a reservoir containing 30 wt.% aqueous KOH (Figure 8(c)). Configuration-2 demonstrated higher reproducibility compared to Configuration-1. Using this configuration, six different Ni-based substrates; Ni mesh, Ni perforated plate, fine Ni foam (compressed and uncompressed), and coarse Ni foam (compressed and uncompressed) were systematically evaluated as both anode and cathode electrodes. The corresponding electrode microstructures are shown in Figure 9.

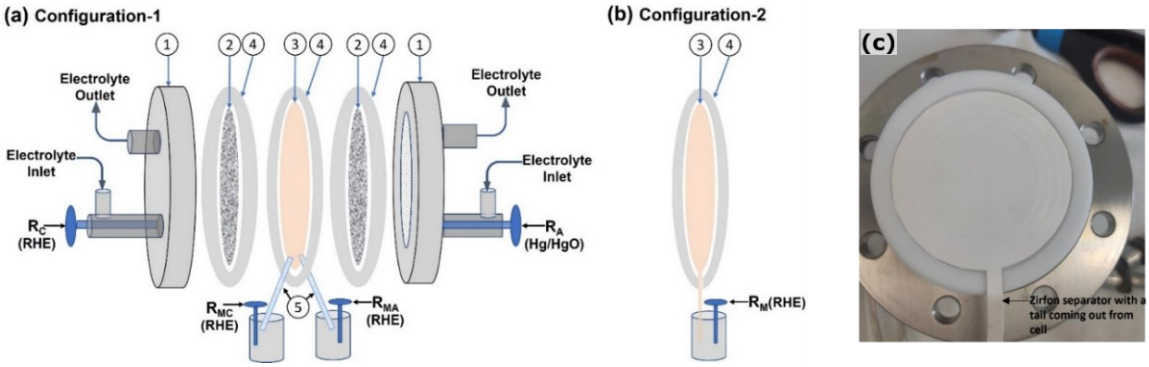

Figure 8. Schematic of the flow cell and reference electrode placement configurations. (a) Configuration-1: two reference electrodes (R_{MC} and R_{MA}) connected to the separator/electrode interfaces via microporous PES membrane strips, (b) Configuration-2: modified separator with an extended strip providing ionic contact to a single external reference electrode (R_M) and (c) Photograph of separator placement in Configuration-2. Components: (1) cell housing end plates, (2) nickel electrodes, (3) Zirfon separator, (4) PTFE gaskets, and (5) microporous PES membrane strips.

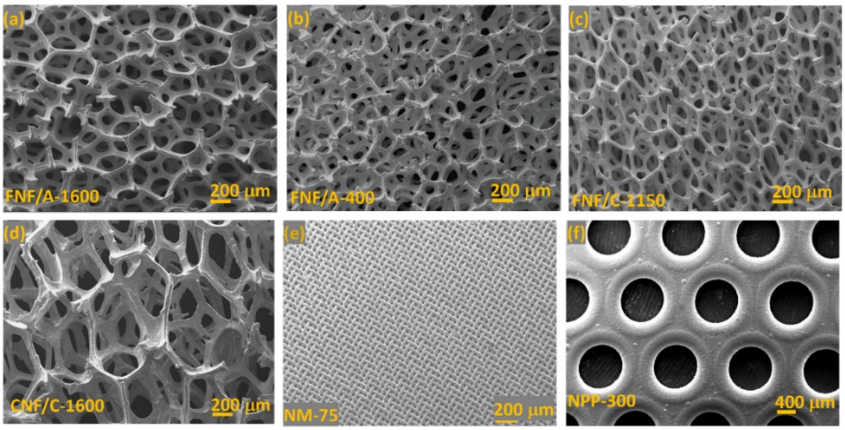

Figure 9. Electron microscopy images of (a) FNF/A-1600, (b) FNF/A-400, (c) FNF/C-1150, (d) CNF/C-1600, (e) NM-75 and (f) NPP-300 electrodes. Images of all the samples are shown at 100x magnification except the NPP-300 which is shown at 50x magnification. FNF is fine Ni foam (NF), CNF is coarse NF, NPP is Ni perforated plate and NM is Ni mesh. Numbers represent support thickness along with supplier. FNF/A-1600 represents 1600 µm thick fine NF from Alantum corp., whereas FNF/C-1150 represents 1150 µm thick fine NF from from Celmet corp.

The placement of multiple reference electrodes allowed us to decouple the electrochemical performance of Anode and Cathode. The electrochemical performance of these six structures suggested that a more open structure with large pores is favorable for the OER whereas a higher surface area is beneficial for the HER, as shown in Figure 10.

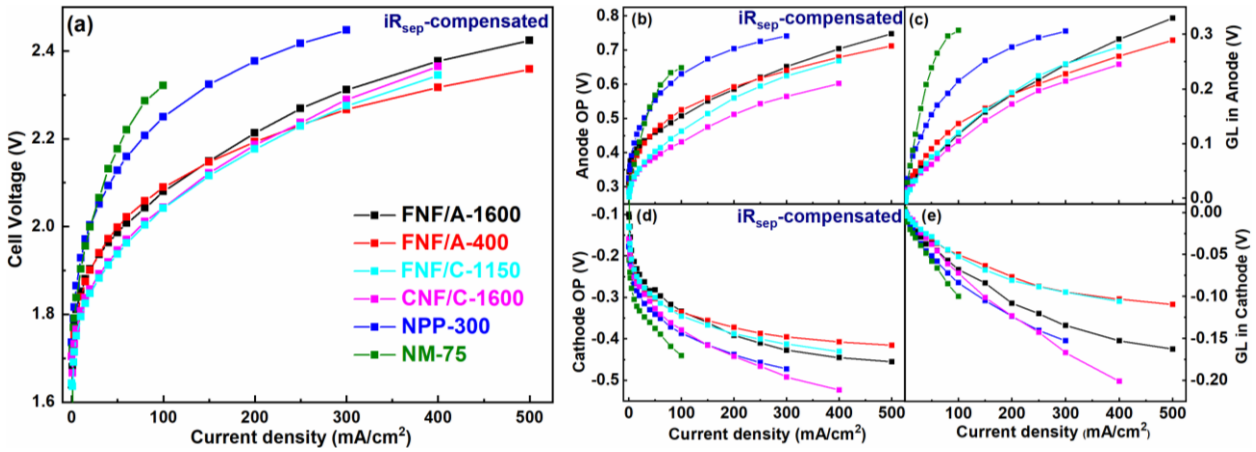

Figure 10. (a) i-V characteristic of six different sets of Ni electrodes used as anode and cathode in symmetric cells tested at room temperature in 30 wt.% KOH. Overpotential of (b) anode and (d) cathode, and corresponding Galvani losses (GL) in (c) anode and (e) cathode.

Our previous studies showed that although the Ni_3Fe_1OOH catalyst initially contains a high amount of Fe, less than 2% is retained after electrochemical testing in 30 wt.% KOH at 80 °C (as determined by EDS). The excess Fe tends to leach into the electrolyte and deposit at the cathode, possibly accelerating cathode degradation over time. To address this issue and develop a more stable anode with reduced Fe content, the Fe at.% in the precursor for hydrothermal synthesis was systematically varied using four Ni:Fe ratios: 75:25, 90:10, 95:5, and 98:2. The resulting electrodes were labeled NiFe-25, NiFe-10, NiFe-5, and NiFe-2, where the number indicates the Fe at.% in the precursor solution. Perforated Ni plates were used as substrates instead of 3D foams, as their 2D structure allows more uniform coatings and ensures better reproducibility in the initial trials.

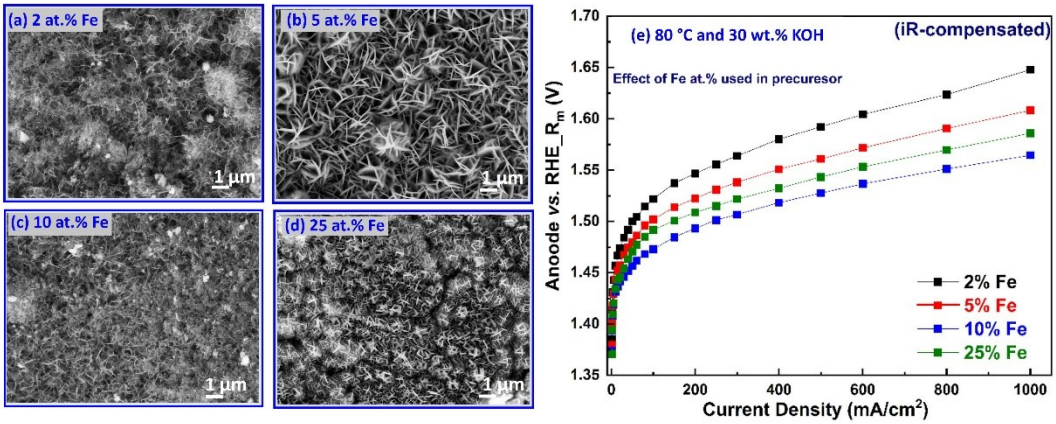

Figure 11. SEM images of NiFeOOH electrodes synthesized with varying Fe content in the precursor: (a) 2 at.%, (b) 5 at.%, (c) 10 at.%, and (d) 25 at.% Fe; (e) corresponding electrochemical performance of the electrodes in 30 wt.% KOH at 80 °C.

SEM analysis of the NiFe samples shows dependence of morphology on Fe content in the precursor as shown in Figure 11 (a-d). At very low Fe content (2 at.%), thin nanoflakes with a highly porous structure were observed. Increasing the Fe content to 5 at.% resulted in a more uniform distribution of nanoflakes, while at 10 at.% the nanoflakes became smaller and tended to form clusters. Further increasing the Fe content to 25 at.% produced platelet-like structures. The electrochemical performance of these electrodes was evaluated in a flow cell with 30 wt.% KOH (Fig. 11e). The electrode Performance improved as Fe content increased from 2 to 10 at.%, but declined as the Fe content further increased to 25 at.%. Based on this optimization, the electrode with 10 at.% Fe was selected for further studies on different Ni supports, including Ni mesh (10 µm and 80 µm openings), expanded Ni sheet, and Ni foam (fine and coarse). These electrodes were tested in a flow cell using a Zirfon220 separator and a PGM-coated perforated Ni (PGM/Ni) cathode supplied by GHS. PGM/Ni cathodes were used throughout the study because GHS was reluctant to share their proprietary cathodes, although their performance was found to be slightly superior to PGM/Ni.

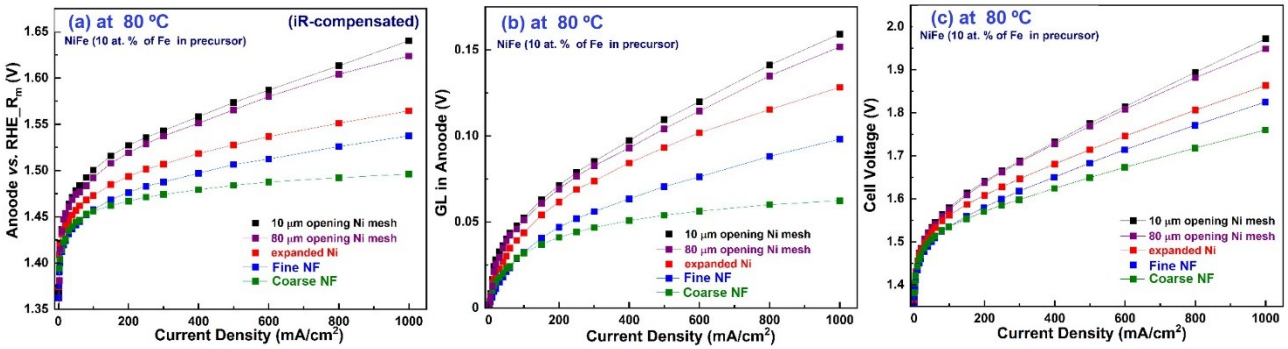

Figure 12. Electrochemical performance of NiFeOOH electrodes prepared on various Ni supports with 10 at.% Fe in the precursor: (a) anode potential vs. RHE, (b) corresponding Galvani loss in anodes and (c) full cell voltage.

The electrochemical performance of the NiFeOOH-coated electrodes followed the same trend observed for the bare Ni supports, where more open structures favored the OER activity. The NiFeOOH coated substrates performed as: Ni foam (NF) > expanded Ni > Ni mesh. Within the NF supports, the coarse foam with larger pores outperformed the fine foam. This enhancement is attributed to reduced Galvani loss (Fig. 12b), indicating improved ionic transport at high current densities. The NiFeOOH-coated coarse NF electrode achieved an overpotential of 265 mV at 1 A cm^{-2} in 30 wt.% KOH at 80 °C. When used with a Zirfon220 separator and a PGM/Ni cathode, this electrode delivered a full-cell voltage of 1.75 V at 1 A cm^{-2}, thereby surpassing the targeted performance.

Long-term testing and degradation studies

During the initial efforts to develop a stable NiFeOOH catalyst coating at DTU, long-term stability tests were initiated at GHS. As shown in Figure 13, two Ni_3FeOOH anodes (one coated on expanded Ni sheet and the other on coarse NF) were tested with a PGM cathode and Zirfon500 separator for 1000 h at 100 °C. The cell voltage profile shows that most of the degradation occurred within the first 24 h, after which the electrodes reached a steady state with a relatively low degradation rate. The cell with NiFeOOH on expanded Ni as anode showed higher activity than on coarse NF; however, its degradation rate was greater (50 mV/1000 h, ~2.5%) compared to coarse NF (20 mV/1000 h, <1%). At this initial stage of testing, both the activity and stability of the electrodes were still below the targeted milestone. Post-mortem analysis further revealed a significant reduction in Fe content, with only 1.1% Fe remaining in the electrode as shown in **Figure 14.** Subsequent efforts were focused on developing NiFeOOH electrodes with lower Fe content, as shown in Figure 11 and discussed previously.

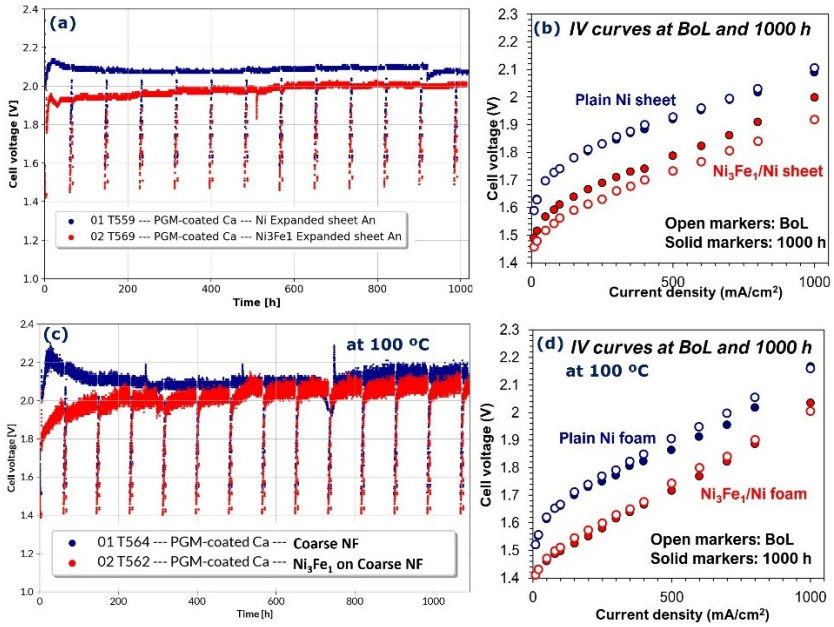

Figure 13. Long-term performance evaluation of the Ni_3Fe_1OOH catalyst coated on (a) expanded Ni sheet and (c) coarse Ni foam (NF), using PGM/Ni as the cathode at 100 °C, with the corresponding i–V curves shown in (b) and (d).

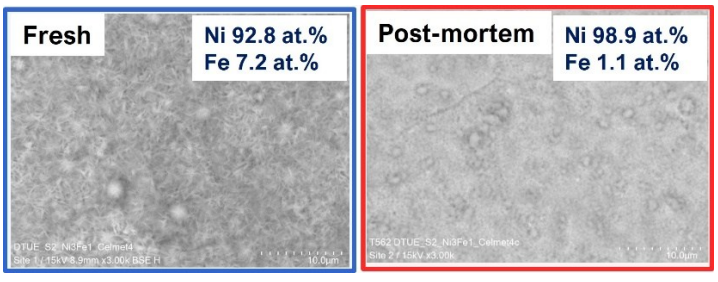

Figure 14. SEM and EDS analysis of as prepared and long-term (1000 h) electrochemically tested NiFeOOH/NF electrode.

$Ni_{1-x}Fe_xOOH$ coatings with varying Fe content, grown on expanded Ni sheet, as well as a 10 at.% Fe containing $Ni_{1-x}Fe_xOOH$ coating grown on different supports (Ni mesh, expanded sheet and Ni foam), were tested to

assess their long-term stability at 80 °C at DTU. The testing protocol consisted of two stages. First, the electrodes were operated under steady-state conditions at constant current densities of 100 mA·cm⁻², 400 mA·cm⁻², and 1 A·cm⁻², each maintained for three days. This was followed by an accelerated stress test under dynamic operating conditions, where the current was cycled between 1 A·cm⁻² (on state) and approx. -1 mA·cm⁻² (off state). The cycling sequence involved: 250 cycles with 2 min on / 30 s off, 250 cycles with 2 min on / 1 min off, and finally 500 cycles with 2 min on / 2 min off. During steady-state operation, all electrodes showed stable performance, as shown in Figure 15 (a–d). However, under dynamic operation, the cell voltage remained stable only during the initial cycling stage where the off time was limited to 30 s, as shown in Figure 15 (e-g). With the increase in off-time, significant degradation of the anode was observed, linked to the decrease of the anode potential to values below approx. 1.25 V vs RHE (related to the $NiOOH/Ni(OH)_2$ reduction potential). Similar degradation trends were observed for all other $Ni_{1-x}Fe_xOOH$ electrodes. However, electrodes with more Fe content appeared less degraded electrochemically. The i-V curves shown in Figure 15(h) also confirm that the electrode performance was stable during constant current operation but degraded under dynamic operation.

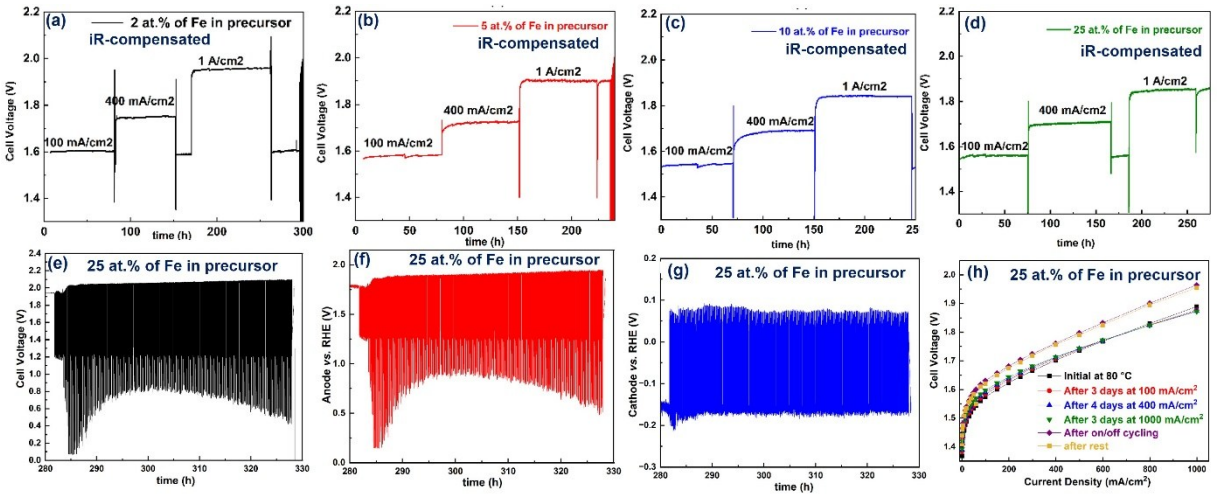

Figure 15. Electrochemical performance of $Ni_{1-x}Fe_xOOH$ electrodes prepared with Fe contents of (a) 2 at.%, (b) 5 at.%, (c) 10 at.%, and (d) 25 at.% in the precursor. Dynamic operation results of the 25 at.% Fe electrode are shown as (e) full-cell voltage, (f) anode potential, (g) cathode potential, and (h) i–V curves recorded at regular intervals

Since the anode was losing Fe during dynamic operation, and the electrode prepared with higher Fe content (NiFe-25) showed reduced degradation, we hypothesized that the addition of Fe in the electrolyte could improve anode stability, establishing a dynamic steady state between Fe dissolution and redeposition with reduced loss of Fe from the anode coating. To test this, we introduced 1 ppm Fe into the electrolyte at the start of the experiment. We compared two cells with NiFe-10 catalyst on coarse NF as anode and PGM/Ni as cathode in 30 wt.% KOH, with and without Fe addition. The presence of 1 ppm Fe in the electrolyte showed indeed suppressed anode degradation after dynamic operation (1000 on/off cycles). On the other hand, when the cell voltage was decoupled into anode and cathode contributions, the cathode was also found to be degraded significantly in the Fe-containing electrolyte (~30 mV increase in cathode potential at 1 A/cm²), whereas in the Fe-free test, the cathode degradation was minor (~7 mV increase in cathode potential at 1 A/cm²).

In parallel, long-term testing of selected electrodes was conducted at GHS under steady-state conditions by operating the cell at constant current densities of 100 mA·cm⁻², 400 mA·cm⁻², and 1 A·cm⁻² for five days each. Subsequently, the cell temperature was increased from 80 to 100 °C, and testing continued at 1 A·cm⁻² for 1000 hours. Consistent with the results obtained at DTU, the electrodes demonstrated stable performance. As shown in Figure 16, four types of anodes - bare Ni and $Ni_{1-x}Fe_xOOH$ coated Ni (containing 2, 5, and 10 at.%

Fe) supported on expanded Ni - were evaluated with a PGM/Ni cathode in 30 wt.% KOH using a Zirfon 500 separator. All electrodes showed stable cell voltages at 80 °C. Notably, the NiFe-10 anode showed an activation effect, with ~40 mV reduction in cell voltage when held at 1 A·cm^{-2} at 80 °C. At 100 °C, the cell with the NiFe-2 anode maintained a constant voltage, while the cells with NiFe-5 and NiFe-10 anodes showed ~5 mV increase suggesting a combined cell degradation at a rate of ~0.25% per 1000 h. Decoupling of electrode contributions was not implemented at GHS; it is therefore not possible to tell how this degradation is distributed amongst the two electrodes.

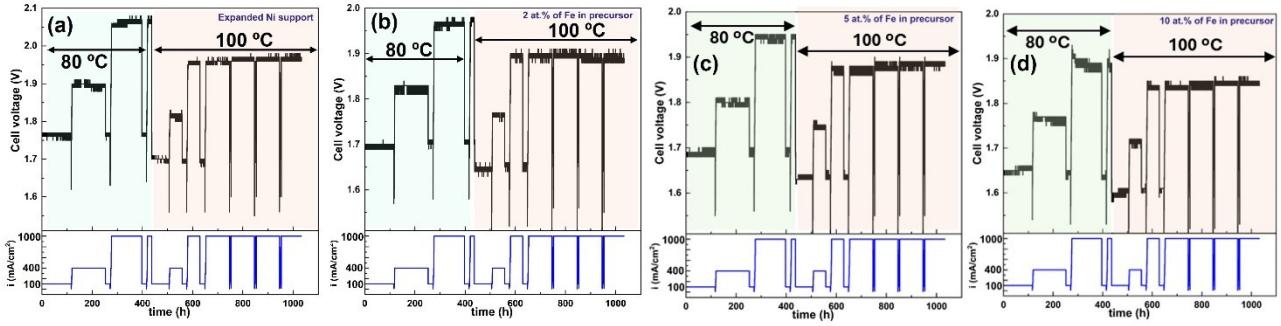

Figure 16. Long-term electrochemical performance of (a) expanded Ni support and $Ni_{1-x}Fe_xOOH$ electrodes prepared with (b) 2 at.% Fe, (c) 5 at.% Fe, and (d) 10 at.% Fe. All tests were conducted using a PGM/Ni cathode and a Zirfon 500 separator.

Despite showing stable operation under long-term testing of 1000 h, the post-mortem SEM images of these electrodes show microstructural changes as shown in Figure 17. The highly porous coating consisting of an interconnected array of nano flakes appears substantially altered into an inhomogeneous layer of particles. This suggests the need for even longer testing to conclude on the commercial viability of this electrode.

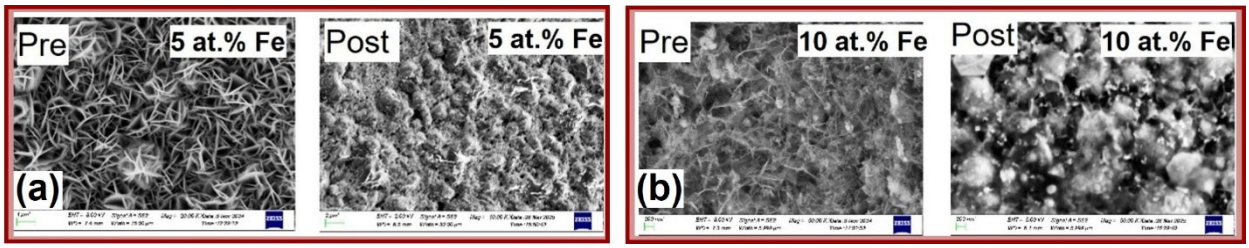

Figure 17. SEM images of as-prepared and electrochemically tested $Ni_{1-x}Fe_xOOH$ electrodes prepared with (a) 5 at.% of Fe and (b) 10 at.% of Fe in the precursor.

Multiphysics simulations:

A computational fluid dynamics model of an alkaline electrolyzer was developed at AAU Energy in collaboration with GHS. In the end of the project, the model had world-leading capabilities. In detail, it included:

- A multi-fluid approach that employed a full set of conservation equations for each phase, thus allowing for the simulation of bubble movement and the increase in ohmic resistance owing to the gas phase which inhibits liquid phase transport.
- The Butler-Volmer equation on each electrode to calculate the electrolyzer performance. This three-dimensional electrode model provides an important link to the work conducted at other project partners. Several key parameters for the prediction of the electrolyzer performance were included, such as the electrode porosity and specific surface area of the catalyst (catalyst morphology), the electrochemical transfer coefficients and activation energies (catalyst type), hydrophilic and hydrophobic pore fractions (catalyst treatment/composition). The calculated performance curves showed a good – but

not excellent – agreement with experimental data, suggesting that more work is needed to obtain a deeper understanding of the underlying transport processes.

- Crossover data for hydrogen and oxygen was used to validate the model with very good results. The model can calculate the amount of hydrogen in oxygen and vice versa. Obviously, these values should be as low as possible, but the observation was that the crossover rates in experiments were much higher than the model originally predicted. A thorough analysis led to the understanding that the liquid electrolyte phase is highly supersaturated, meaning that more hydrogen and oxygen is dissolved in the liquid phase than thermodynamic equilibrium calculations would predict. This led to the understanding that the liquid phase could be de-gassed, and the amount of hydrogen and oxygen crossover would then decrease drastically. In collaboration, AAU Energy and GHS submitted an invention disclosure that described the possibility of inserting micro-cracks in the diaphragm. This was meant to lead to bubble formation and thus decrease the crossover rate. In unrelated research, a consortium of DTU Energy and Stiesdal A/S has measured and published that the introduction of micro-cracks in an alkaline electrolyzer diaphragm leads to drastic crossover reduction. Thus, we know that our invention works.
- The model is non-isothermal, thus allowing for the prediction of the temperature change in the electrolyzer.
- The model was used to study both a finite-gap design and a zero-gap design of an alkaline electrolyzer which was according to the original project plan.
- The model was used to study the complex 3D geometry of a laboratory scale alkaline electrolyzer from DTU with round plates and pins, kindly loaned to us from DTU. However, this was at the end of the project, and the experiments conducted by the PhD student at U. Canterbury, New Zealand, were highly time demanding, thus we could not complete simulations on the complex geometry.

In the following, sample results of the final model version are shown, published in the prestigious Journal of the Electrochemical Society (JES) (“Eulerian-Eulerian CFD Modeling of Multiphase Flow and Heat Transfer in Alkaline Electrolysis Cells”, JES 172 064501, 2025).

Figure 18 shows the computational mesh that was used after a so-called grid refinement study had been conducted. Once finalized, the model included two phases, gas and liquid, in a so-called Eulerian approach where a complete set of transport equations was solved for each phase. In addition, the model accounted for the species hydrogen and oxygen, and it was tracking hydronium ions to calculate the electrical field both in the electrolyte phase and the solid current collectors. A comparison of the calculated performance curve showed good agreement with experiments taken from the literature, and it was concluded that the main physics had been captured, see Figure 18.

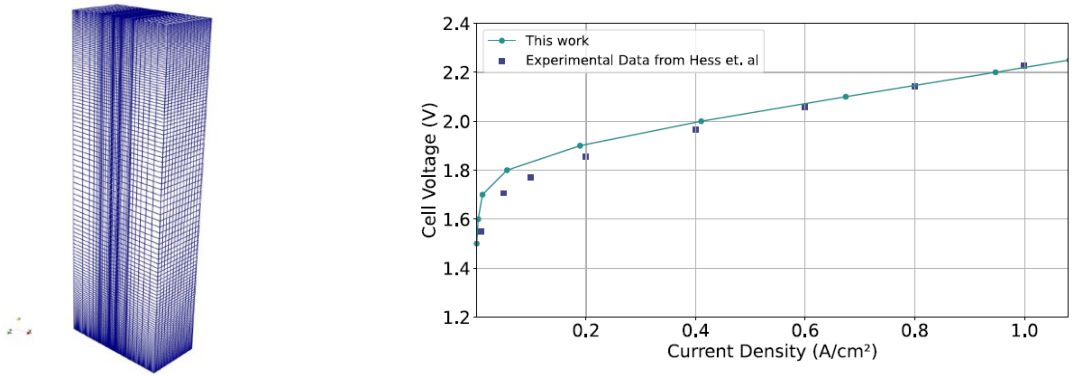

Figure 18. Computational mesh including the negative current collector, porous cathode, diaphragm, porous anode and positive current collector (left), and the calculated polarization curve including comparison with the literature (right).

A parametric study was conducted to better understand the role of the electrolyte concentration as well as the role of the operating temperature. There were no detailed experimental data available at the time, and therefore these results are merely of indicative nature, demonstrating the model capability. The model is also capable of calculating the anode and cathode activation overpotentials according to the Butler-Volmer equation. This equation represents the important link between the catalyst characterization conducted at DTU and GHS and our model, as we require input parameters such as catalyst layer porosity and tortuosity, activation energy, transfer coefficients, and possible degradation rates. The calculated activation overpotentials based on literature values is input parameters are shown in Figure 19, right.

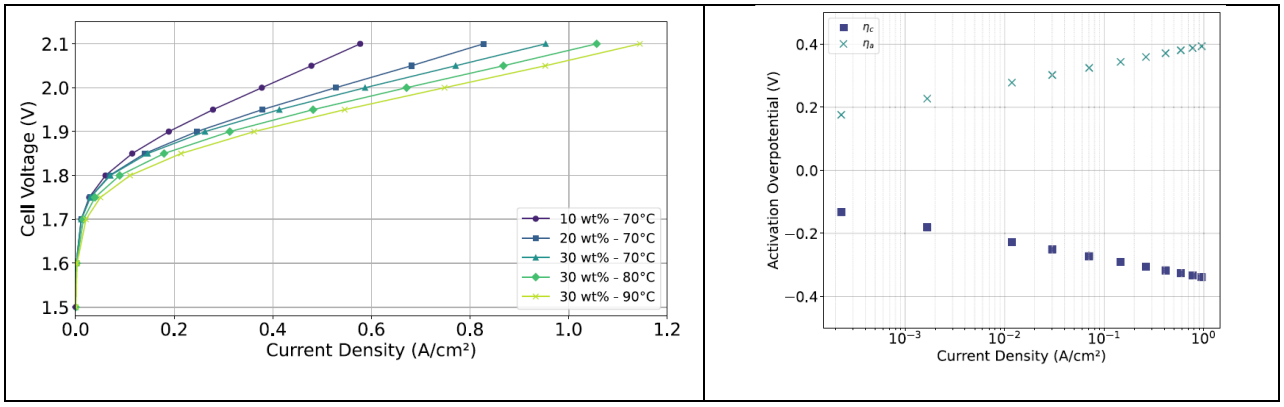

Figure 19. Predicted electrolyzer performance as function of the electrolyte concentration and temperature (left) and the calculated activation overpotentials according to the Bulter-Volmer equation (right).

Among the further unique features is the fact that the model is non-isothermal, allowing for the prediction of the temperature change. However, so far, only small domains have been investigated, and therefore the temperature increase is very modest, around 1 °C.

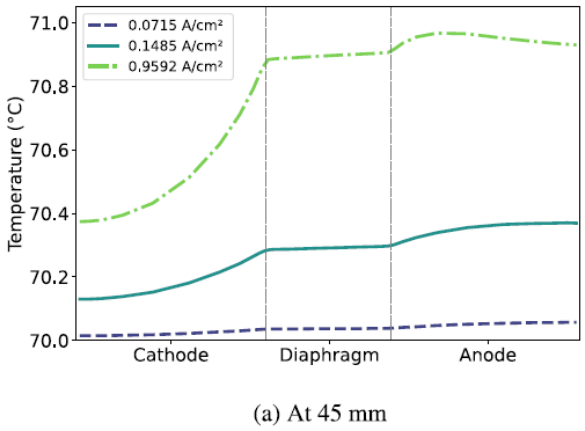

(a) At 45 mm

Figure 20. Calculated temperature distribution along the channel position of 45 mm for three different current densities.

Calculated gas volume fraction is shown in Figure 21 for two different current densities, I =0.5927 A/cm^2 and I = 0.9687 A/cm^2. On the left-hand side in each plot, one can see the higher volume fraction of the hydrogen which is produced at twice the rate as oxygen, and the volume fractions both increase with current. These values have been compared with results from a research group from South Korea, and they matched exactly.

Finally, in order to validate the model, experiments were conducted at GHS to measure the so-called crossover rate, i.e. the amount of hydrogen that ends up at the oxygen side and vice versa. A reduction of the crossover

rate will widen the operating window towards lower current densities and thus allow higher efficiencies and a better coupling of electrolyzer technologies to the fluctuating wind and solar input power.

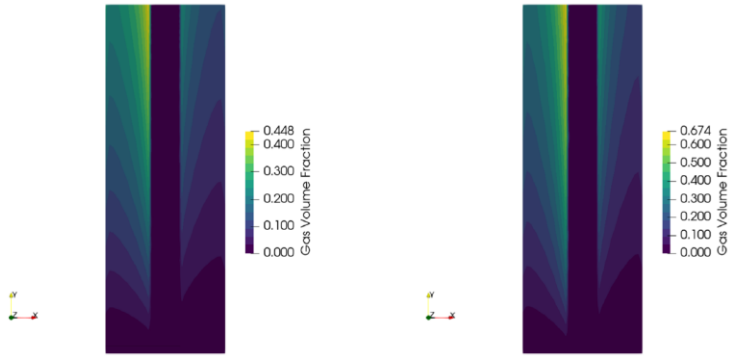

Figure 21. Calculated gas volume fraction distribution inside the hydrogen compartment (left side) and the oxygen compartment (right side) for two different current densities.

Figure 22, left shows a comparison between experimental data (reduced order model, ROM) and the model, not permitting the liquid phase to be supersaturated with either oxygen or hydrogen (ψ=1). The numerical model was unable to capture the major trend observed from experiments. When allowing the liquid phase to be supersaturated with dissolved gases, the experimental trend could very well be matched (see right side for ψ=20). From this, we could conclude that the liquid phase in the alkaline electrolyzer is supersaturated with the product gases, and if we would be able to degas the liquid phase, we could drastically reduce the amount of crossover.

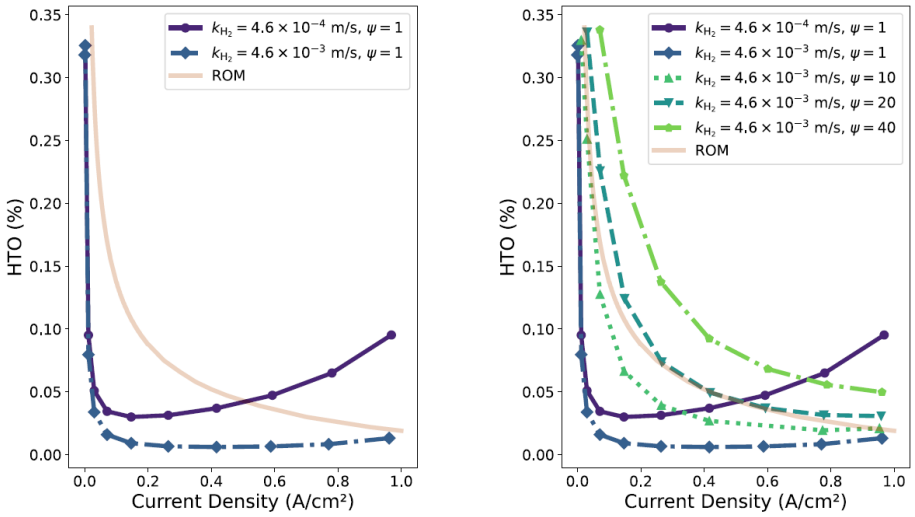

Figure 22. Comparison of crossover data between experiments (reduced order model – ROM) and modeling results without supersaturation (left) and with supersaturation (right).

We then finally proposed to try and degas the liquid phase by introducing cracks into the diaphragm membrane, as it is a known effect that such cracks can cause gas bubbles and thus lead to a degassing of the liquid phase. This part was submitted as an invention disclosure and later published.

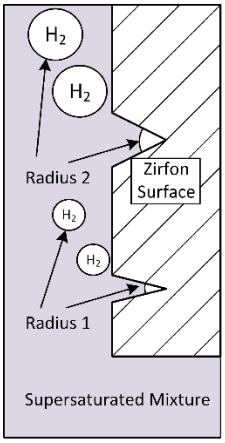

Figure 23. Proposed modification of the membrane morphology including cracks to induce the formation of gas bubbles and thus lead to a reduction in crossover.

Stack design:

A flow-optimized cell frame for the electrolysis stack was designed, based on simulation results from WP3. It was successfully tested, showing better flow distribution and thus also temperature distribution across the cell/stack. Unfortunately, GHS entered the in-court reconstruction process before finishing and analysing this data. GHS was also not able to give out the data to project partners and were not able to work on finalizing the analysis themselves.

On a similar note, GHS produced a full scale stack with ø30cm cells, incorporating the improved electrodes and cell frame design, and it was installed for testing but not turned on before entering into in-court reconstruction, after which they had to interrupt any further activities.

There were no commercial results obtained as GHS went bankrupt before being able to capitalize on their alkaline water electrolysis technology and the incorporation of the innovations achieved through BEEST2.

It is nevertheless expected that other AWE developers will be able to obtain some of GHS' IP and knowhow. Furthermore, the technological developments and knowhow generated at DTU and AAU are expected to be of interest to other AWE developers and electrode producers who will engage in further maturing these results towards commercial exploitation in the future.

The project results have been disseminated through scientific publications to international peer reviewed journals and though oral and poster presentations at scientific conferences, as listed below.

Scientific publications to international peer reviewed journals:

P. Leuaa, M. R. Kraglund, and C. Chatzichristodoulou, "Decoupling of Reaction Overpotentials and Ionic Transport Losses within 3D Porous Electrodes in Zero-Gap Alkaline Electrolysis Cells", Electrochim. Acta, 2023, 470, 143306

D. L. Martinho, T. Berning, M. Abdollahzadehsangroudi, A. Rasmussen, J. Hærvig, S. S. Araya: "A Three-Dimensional, Multiphysics Model of An Alkaline Electrolyzer", ECS Transactions. 112, 4, 433-447 16, 2023.

S. Iqbal, J. C. Ehlers, I. Hussain, K. Zhang, C. Chatzichristodoulou, "Trends and industrial prospects of NiFe-layered double hydroxide for the oxygen evolution reaction", Chem. Eng. J., 2024, 499, 156219.

D. L. Martinho, M. Abdollahzadehsangroudi, T. Berning: "Computational Fluid Dynamics Analysis of Gas Crossover in an Alkaline Electrolyzer Using a Multifluid Model", ECS Transactions. 114, 5, 727-739, 2024.

P. Leuaa, Y. A. Farzin, S. Iqbal, C. Chatzichristodoulou, "Cobalt oxide (CoOx) coated Ni foam anodes for high temperature (150 °C) and pressure (45 bar) alkaline electrolysis", J. Power Sources, 2025, 625, 235625

D. L. Martinho, M. Abdollahzadehsangroudi, S.S. Araya, T. Berning: "Eulerian-Eulerian CFD Modeling of Multiphase Flow and Heat Transfer in Alkaline Electrolysis Cells", J. Electrochem. Soc. 172 (6), 064501, 2025.

D. L. Martinho, T. Berning: "A Conceptual Approach to Reduce the Product Gas Crossover in Alkaline Electrolyzers", Membranes 2025, 15(7), 206; (Open Access). https://doi.org/10.3390/membranes15070206 - 12 Jul 2025

T. Berning, D. L. Martinho: "An alkaline electrolyzer having a diaphragm surface coating to enable bubble formation and thus reduce the crossover rates of the product gases", Invention Disclosure, Vol. 5, December 2025, 10004 (Open Access). https://www.sciencedirect.com/science/article/pii/S2772444125000072.

Scientific conference participation:

ICE 2023 – 4th International Conference on Electrolysis, "Integration of Reference Electrodes in Zero-Gap Alkaline Electrolysis Cells for the Deconvolution of Reaction Overpotentials and Ionic Transport Losses Across the Anode, Cathode, and Separator", P. M. Leuaa, M. R. Kraglund, and C. Chatzichristodoulou, August 27 - September 1, 2023, Sun City, South Africa. Oral presentation,

ICE 2023 – 4th International Conference on Electrolysis, August 27.-September 1., 2023, Sun City, South Africa, (https://engineering.nwu.ac.za/hysa/ice-2023). Oral Presentation.

Annual Meeting of the Danish Electrochemical Society, "Analysis of overpotentials and ionic transport losses across the zero-gap alkaline electrolysis cells", P. M. Leuaa, M. R. Kraglund, and C. Chatzichristodoulou, November 2-3, 2023, Lyngby, Denmark. Oral presentation,

244th Meeting of the Electrochemical Society, October 8-12, 2023, Gothenburg, Sweden. (https://www.electrochem.org/244). Oral presentation.

246th Meeting of the Electrochemical Society, PRiME 2024, October 6-11, 2024, Honolulu, Hawaii, USA. (https://www.electrochem.org/prime2024). Oral presentation.

Indo-Danish Battery and P2X Alliance Webinar on Electrolyser Technology, "Material Innovation For Inexpensive High Performance Electrolyzers", C. Chatzichristodoulou et al, April 30, 2025. *Oral presentation,*

ICE 2025 - 5th International Conference on Electrolysis, "Accelerating Electrocatalyst Development and Electrode Architecture Optimization for Advanced Alkaline Electrolysis", C. Chatzichristodoulou et al, August 25-29, 2025, Freiburg, Germany. *Oral presentation,*

Indo-Danish Research Alliance Conference on Battery and P2X Technologies, oral presentation, "Accelerating Electrocatalyst Development and Electrode Architecture Optimization for Advanced Alkaline Electrolysis", C. Chatzichristodoulou et al, 1-3 September, 2025, Lyngby, Denmark

ICAE 2025 – 8th International Conference on Advanced Electromaterials, oral presentation, "Accelerating Electrocatalyst Development and Electrode Architecture Optimization for Advanced Alkaline Electrolysis", C. Chatzichristodoulou et al, November 25-28, 2025, Jeju, Korea

6. Utilisation of project results

- *Describe how the obtained technological results will be utilised in the future and by whom.*
- *Describe how the obtained commercial results will be utilised in the future and by whom the results will be commercialised.*
  - *Did the project so far lead to increased turnover, exports, employment and additional private investments? Do the project partners expect that the project results in increased turnover, exports, employment and additional private investments?*
- *Describe the competitive situation in the market you expect to enter.*
  - *Are there competing solutions on the market? Specify who the main competitors are and describe their solutions.*
- *Describe entry or sales barriers and how these are expected to be overcome.*
- *How does the project results contribute to realise energy policy objectives?*
- *If Ph.D.'s have been part of the project, it must be described how the results from the project are used in teaching and other dissemination activities.*

The unfortunate turn of events with GHS declaring bankruptcy did not permit the drafting of a concrete plan for utilization of project results. Nevertheless, the technological developments achieved at DTU and AAU represent a solid step forward and can form the basis for future commercial developments at other AWE developers.

DTU

The established methodology for decoupling electrode contributions during zero-gap flow-cell testing offers a very powerful tool in the effort to optimize electrode and flow-field architectures and in understanding degradation patterns at industrially relevant operating conditions. There is no doubt that this methodology will help accelerate progress in the development of more efficient and durable electrodes for AWE, as it is already proving its potential and is gradually being taken up by other research groups in the field.

Within BEEST2, this methodology helped identify porous Ni support architectures with excellent performance as AWE anodes when coated with an optimized $Ni_{1-x}Fe_xOOH$ catalytic coating. When combined with a commercially available PGM coated Ni cathode (or a PGM free GHS Cathode) and a commercial Zirfon220 diaphragm, a current density of 1 A cm^{-2} could be achieved at a full-cell voltage of 1.75 V at 80 °C, 1 bar in 30 wt% KOH with negligible degradation upon continuous polarization over 1000h long tests, thereby surpassing the EU Clean Hydrogen SRIA targeted performance for 2030 (1 A cm^{-2} at 1.8 V with degradation of 0.1%/1000h). Despite the apparent electrochemical stability, drastic microstructural and compositional changes were observed in post-mortem analysis, requiring even longer-term testing to assess their commercial potential in industrial applications.

AAU

It must unfortunately be stated that owing to the bankruptcy of GHS, the modeling part of the project will probably be lost. The original goal from both GHS and AAU Energy was to establish a long-term collaboration where BEEST2 would only be the start. The computational model, based on the commercial software package ANSYS Fluent, has by now some world-leading capabilities, and it is at par with research

efforts at FZ Jülich, Germany, where a similar model based on the open software Open FOAM was developed over the course of more than 15 years. However, the PhD student at AAU, Diogo Loureiro Martinho, was the only user of ANSYS Fluent at GHS, and thus the only person that can run the computational model. Moreover, it is common knowledge that only the code developer knows the model in full. Therefore, it is unlikely that this model can be run by anybody else in the foreseeable future. While in the beginning of the project, GHS asked the student to commit to working with GHS after the project was ended, the bankruptcy obviously prevented such employment. The student has found a very good job with Novo Nordisk and is unlikely to return to electrolyzer modelling.

The Invention Disclosure "An alkaline electrolyzer having a diaphragm surface coating to enable bubble formation and thus reduce the crossover rates of the product gases", submitted in the beginning of February 2024, was not followed up upon. While GHS first declared commercial interest in our invention (it was 50:50 between AAU and GHS), they decided, in agreement with the AAU Technology Transfer Office, to not further pursue this idea.

7. Project conclusion and perspective

DTU

The electrode development efforts have helped consolidate a method for decoupling of electrode performance contributions within an AWE cell operating within an industrially relevant setting. This is extremely advantageous both with respect to electrode performance optimization efforts as well as with respect to assessing and understanding electrode degradation. There is no doubt that this development will help accelerate progress in the field.

Furthermore, BEEST2 contributed to identifying HER and OER electrocatalysts holding great promise in terms of both activity and durability in AWE. It also enabled the screening of a selected range of electrode architectures, identifying general trends in terms of required characteristics for well performing Cathode and Anode architectures. Combining selected catalyst coatings and architectures yielded cells that could deliver 1 A cm^{-2} at a full-cell voltage of 1.75 V at 80 °C, 1 bar in 30 wt% KOH, surpassing the EU Clean Hydrogen SRIA target performance for 2030 (1 A cm^{-2} at 1.8 V). Further improvements in performance may be anticipated in future efforts upon further exploitation of identified trends.

The long-term evolution of the employed $Ni_{1-x}Fe_xOOH$ catalyst coatings was thoroughly investigated. It is a complex function of catalyst composition, electrolyte purity, and operational profile. Although negligible degradation was observed upon continuous polarization over 1000 h long tests at 80-100 °C in 30 wt% KOH, post-mortem analysis revealed drastic microstructural and compositional changes. Even longer-term testing is therefore required to assess the industrial viability of these electrodes.

Intermittent operation proved to be detrimental to the developed anodes but linked to the instability of the interface between catalytic coating and porous Ni support rather than the catalytic coating itself. Further efforts are required in the direction of understanding and tuning this interface for intermittent operation.

AAU

This was our first exposure to alkaline electrolyzer technology in general. Our own prior focus had been on the development of a proton exchange membrane electrolyzer. We do consider our part of the project to be highly successful. A PhD student was educated and completed his PhD in three years, and his work led to several publications and one invention disclosure where we know by now it works in principle, thus probably advancing

alkaline electrolyzer technology. From a Danish perspective, part of the inventions and discoveries might be picked up by Stiesdal A/S. The PhD student, originally from Portugal, has started a good position in the modelling department of Novo Nordisk, thus contributing to the Danish Society. The computational model could be further developed, but because for reasons stated above, this is unlikely to happen, which is a pity because our model is second to none, and it is important to have an in-house model.

Overall, we very much appreciated GHS contacting us in 2021 and suggesting to collaborate based on CFD modelling, and we are sad and disappointed about the bankruptcy of GHS. We explicitly want to thank Anders Rønne Rasmussen and Ahsan Iqbal from GHS for inviting us to collaborate on this exciting technology.

8. Appendices

P. Leuaa, M. R. Kraglund, and C. Chatzichristodoulou, "Decoupling of Reaction Overpotentials and Ionic Transport Losses within 3D Porous Electrodes in Zero-Gap Alkaline Electrolysis Cells", Electrochim. Acta, 2023, 470, 143306

S. Iqbal, J. C. Ehlers, I. Hussain, K. Zhang, C. Chatzichristodoulou, "Trends and industrial prospects of NiFe-layered double hydroxide for the oxygen evolution reaction", Chem. Eng. J., 2024, 499, 156219

P. Leuaa, Y. A. Farzin, S. Iqbal, C. Chatzichristodoulou, "Cobalt oxide (CoOx) coated Ni foam anodes for high temperature (150 °C) and pressure (45 bar) alkaline electrolysis", J. Power Sources, 2025, 625, 235625